# On the Kinetics of Palm Oil Crystallisation

Juliet A. Adelakun[1], Xiong-Wei Ni[2*]

EPSRC, Centre for Continuous Manufacturing and Crystallisation (CMAC), Centre for Oscillatory Baffled Reactor Applications (COBRA), School of Engineering and Physical Science, Heriot Watt University, Edinburgh. EH14 4AS, UK
[*]Corresponding author; email: x.ni@hw.ac.uk; Tel: 00441314513781

***Abstract*—** *In this work the crystallisation of palm oil (a typical melt) is used as a model process and kinetic parameters at different end temperatures and cooling rates were evaluated using three model approaches: two from the traditional melt fractionation, one from the classic solution crystallisation. The objective was to establish critical understanding on the various model approaches and their applications. Differential Scanning Calorimetry (DSC) was used to obtain the melting temperatures, isothermal induction times and enthalpy of the crystallisation for the Fisher-Turnbull and Avrami model evaluations, while turbidity and temperature probes were utilized to generate metastable zone width as a function of cooling rates for the classical Nyvlt model analysis. Our results show that the Fisher-Turnbull and the Nyvlt models are useful in estimating the nucleation rate constants (kn) with reasonable agreement: this unites the model approaches and allows comparison between fat fractionation and solution crystallisation of organics. While the Avrami model is capable of evaluating the growth mechanism of the formed crystals (n) and the overall crystallisation rate constant (k), none of the parameters can be compared with other models because of the different definitions of the growth mechanism as well as the dependence of k value on the growth mechanism when dealing different fats of varying compositions. This is the first contribution of this work. In addition, our results indicate that the growth of nuclei to a stable size was generally slower in melt crystallisation compared to a typical organic solution system due to the relatively lower rate constant (kn) and the high viscosity and multicomponent properties of the melt system used in this study. This is the second contribution of this work.*

***Keywords*— Avrami model, Crystallisation, Fisher-Turnbull model, nucleation rate constant, Nyvlt model, palm oil fractionation.**

## I. INTRODUCTION

Crystallisation by cooling is a well-known unit operation used in a wide range of industries from pharmaceuticals to food for product purification, separation and/or recovery. For pharmaceutical ingredients, for example, the purity of the solute out of the solution is a critical product parameter. For edible oils/melts in food industry, on the other hand, it is the purity or the clearness of the solution that matters. Although the terminology of crystallisation is used for all inorganic and organic compounds, while fractionation is applied to all melts, the essence of the process is the same, i.e. by cooling for all. In spite of the similarities in the processes, different model approaches have been used for crystallisation from solution (e.g. APIs) than from melts (e.g. fats). Taking palm oil as the model compound for melt, it consists of a wide range of triglyceride (TAGs) fractions based on their physical state at different temperatures[1] – olein (liquid), mid-fractions (soft solid) and stearin (solid). These are significantly different to crystallisation of paracetamol for instance. The aims of this work are to evaluate and compare kinetics from a melt crystallisation extracted using models for both melts and organics; and to establish critical understanding on the various model approaches and their applications.

### 1.1 The Models

Three models are considered: the first two from traditional melt crystallisation, the last one from solution crystallisation.

The first model for melts is the *Avrami model* dealing the rate of phase change (i.e. the formation of solid phase from liquid phase per unit time) at isothermal conditions. It is a simplistic model that uses the *deterministic*[2] approach to evaluate the *overall* kinetics in relation to nucleation mode and crystal growth mechanism[3, 4] of the isothermal process. The model was developed based on a few assumptions, one of which is that the growth rate is constant throughout the crystallisation process[3]; but this may not be the case for fat systems in practice due to their multicomponent property. Hence modifications to the Avrami model have been proposed by other researchers[5-7]; nevertheless the Avrami model, though simplistic, has widely and successfully been used to characterise the *overall* kinetics of fat crystallisation,[2] that is why it is chosen for this work.

The second model in consideration in this study is the *Fisher-Turnbull (F-T) correlation*, which estimates the activation energy barrier required for the formation of stable nuclei by exploring the relationship between the degree of supercooling and the induction time needed for the formation of the nuclei[8]. Similar to the Avrami approach, there are a few assumptions

for the F-T model, e.g. induction time is a direct indication of nucleation event at a macroscopic level[9, 10]. This assumption is not unreasonable due to the negligibility of some of the inherent steps[11]. The activation energy would allow the nucleation rate constant at isothermal conditions to be determined. Although this method was originally designed for pure systems which is not the case for fat systems, it has widely and successfully been used to characterise the *nucleation* kinetics of fat crystallisation [12]; hence it is adopted for this work.

Since fractionation of fat is effectively a cooling crystallisation process, the *classical Nývlt nucleation theory* is also applicable where the nucleation rate is a function of supersaturation and the rate of supersaturation generation is a function of cooling rate. By measuring the metastable zone width at different cooling rates experimentally, the apparent nucleation order and the nucleation rate constant can be determined and compared with these from the two holistic models.

## II. MATERIALS AND METHOD

### 2.1 Materials

Refined, bleached and deodorised (RBD) palm oil was supplied by AarhusKarlshamn, AAK (Hull, UK). The saturated fat content was 50.8% with palmitic acid forming 44% of the fatty acid assay. The same batch of material was used for all the experiments without further purification. Palm stearin and olein were considered as the two main fractions that constitute the solid and liquid products respectively.

### 2.2 Isothermal Crystallisation

The induction times of crystallisation ($\tau$) and the melting point ($T_m$) were determined with a NETZSCH differential scanning calorimeter (model DSC 214 Polyma, NETZSCH, Germany) equipped with an intracooler cooling system operating between a temperature range of -70 to 600$^o$C. Nitrogen at a flowrate of 40 mL/min and compressed air at a flowrate of 20 mL/min were used as the purge and protective gas respectively. 15–18 mg of sample was weighed into an aluminium pan and sealed with a pierced lid; an empty and sealed pan was used as a reference. The sample was heated to 353K at a rate of 10 K/min and held at this temperature for 10 min. The sample was then cooled to the pre-set end temperature (293 – 301K) at 20 K/min and held at each of the end temperatures for crystallisation to occur. Since the crystallisation is an exothermic process, the onset of the exothermic peak during the isothermal period was taken as the induction time ($\tau$) and all were evaluated using the DSC 214 software. At the end of the crystallisation process, the sample was then heated back to 353K at 10 K/min to obtain the melting curves.

### 2.3 Non-isothermal Crystallisation

To obtain the dynamic thermograms of the palm oil used for this study, the same DSC equipment as above was used; the sample (10 – 15 mg) was heated to 353K for 5 min, then cooled to 223K at the rate of 10 K/min; it was held at this temperature for 5 min to allow complete crystallisation. The sample was then heated again to 353K at the rate of 10 K/min to obtain the melting curve; the melting point ($T_m$) of the palm oil sample was taken as the temperature at the end of the curve, i.e. when melting is completed. This method of the determination of melting point is in accordance to previous works by Dodd & Tonge[13] and Nassu & Goncalves[14].

For the evaluation of the metastable zone width ($\Delta T_{max}$) at different cooling rates, about 400 – 600 mL of palm oil was added to a crystalliser vessel – a DN100 jacketed round-bottom stirred tank fitted with 5-port glass lid and PTFE anchor impeller; the oil was melted at 50$^o$C to ensure complete dissolution and then cooled to 20$^o$C at different cooling rates (0.25 – 1.0 $^o$C/min) at constant mixing condition. GP200-R2 water bath (Grant Inst. Cambridge Ltd) was used to control the temperature of the vessel jacket. Turbidity and temperature (PT100) probes (CrystalEyes system from HEL, UK) were inserted into the crystalliser vessel to monitor and record the cloudiness and temperature of the solution. The system was interfaced with a PC for real-time display, logging and data analysis.

### 2.4 Estimation of kinetic parameters

*The Avrami model*: The basic principle can be illustrated by imagining raindrops falling in a puddle. The raindrops produce expanding circles of waves which intersect and cover the whole surface. The drops may fall sporadically or all at once. In either case, they must strike the puddle surface at random points. The expanding circles of waves are the growth front of the spherulites, and the points of impact are the crystallite nuclei. The original derivations by Avrami[3] have been simplified by

Evans[15] and put into polymer context by Meares[16] and Hay[17]. Through probability derivations[18], the volume fraction of crystalline material, X, known widely as the degree of crystallinity, can be written as:

$$1 - X = e^{-E} \tag{1a}$$

Where E represents the average number of fronts of all such points in the system. For low degrees of crystallinity, a useful approximation is X ≈ E. For the bulk crystallisation of polymers, X in the exponent may be considered the volume or volume fraction of crystalline materials, $V_t$, i.e.:

$$1 - X = e^{-V_t} \tag{1b}$$

This has been the widely accepted and used equation in bulk crystallisation[19-22]. For either instantaneous or sporadic nucleation, equation (1b) can be written as:

$$1 - X = e^{-Kt^n} \text{ or } -\ln(1-x) = kt^n \tag{1c}$$

where ***x*** is the fraction of solid formed at a particular time (***t***); ***k*** the overall crystallisation rate constant; and ***n*** the index of crystallisation, also referred to as the *Avrami exponent*, the phenomenological index of crystallisation[23], depending not only on the structure of the crystal, but also on the nature of nucleation[4, 24]. For example, when *n* = 1, it corresponds to rod-like growth from instantaneous nuclei; whereas *n* = 3 or 4 refers to spherulitic growth from either sporadic or instantaneous nucleation[25]. However, fractional values of *n* also exist due to secondary crystallisation, e.g. lower *n* values (<1) are caused by linear crystal growth[26].

The value of ***x*** was estimated by integrating the isothermal crystallisation exothermic peak from the DSC measurement, as given by the **eq. 2** below where $\Delta H_t$ is the heat of crystallisation (W/g) which is evaluated as the area under the crystallisation curve from the onset of the peak to time *t* using the DSC 214 software; $\Delta H_{tot}$ is the total area under the curve. More detailed description of the methodology can be found elsewhere[27]. The kinetic parameters, ***n*** and ***k,*** were obtained from the slope and the intercept of the plot of [ln(-ln(1–*x*)] against ln(*t*) respectively. The unit of *k* here is the inverse of time to the power of n, depending on the index of crystallisation:

$$x = \Delta H_t \Big/ \Delta H_{tot} \tag{2}$$

The Fisher-Turnbull correlation: This model which was originated by Becker[28] for condensed systems (liquid-solid or solid-solid transformations) links nucleation rate with the activation free energy required for the formation of a stable nucleus and the diffusion energy for phase change. The former (ΔGc) was estimated in the equations below:

$$\frac{1}{J_n} = \tau = \frac{h}{Nk_bT}\exp\left(\frac{-\Delta G_c}{k_bT}\right)\exp\left(\frac{-\Delta G_d}{k_bT}\right)$$
$$-\Delta G_c = \frac{16}{3}\frac{\pi\sigma^3 T_m^2}{(\Delta H \Delta T)^2} \tag{3a}$$

$$T\tau = \frac{h}{Nk_b}\exp\left(\frac{16}{3k_b}\frac{\pi\sigma^3 {T_m}^2}{(\Delta H)^2}\frac{1}{T(\Delta T)^2}\right)\exp\left(\frac{-\Delta G_d}{k_bT}\right) \tag{3b}$$

$$\Delta G_c = \frac{s \times N_A k_b}{(\Delta T)^2} \tag{3c}$$

Where h and $k_b$ are the Planck ($6.626\times10^{-34}$ Js) and the Boltzmann ($1.381 \times 10^{-23}$ $JK^{-1}$) constants respectively; N and $N_A$ are the Avogadro's number and constant ($6.022 \times 10^{23}$ and $6.022 \times 10^{23}$ $mol^{-1}$ respectively); ΔH is the enthalpy of fusion ($Jmol^{-1}$); $T_m$ the melting point of the palm oil (K); ΔT the degree of supercooling ($T_m$ – T) with T being the crystallisation

temperature; s the slope of the plot of ln (Tτ) against 1/T $(\Delta T)^2$ with the unit of $K^3$; $\Delta G_d$ the activation energy for molecular diffusion. Using the activation energy $(\Delta G_c)$ from this model, the nucleation rate constant $(k_n)$ can be estimated based on the Arrhenius-type equation[29] shown below, where *R* is the molecular gas constant (8.314 $Jmol^{-1}K^{-1}$):

$$k_n = A\exp\left(-\Delta G_c / RT\right) \tag{4a}$$

If the rate of solid crystals formation (*dx/dt*) is an indication of the crystallisation rate (*J*), then the rate equation is given as:

$$J = \frac{dx}{dt} = A\exp\left(-\Delta G_c / RT\right) f(x) = k_n f(x) \tag{4b}$$

$$\text{Assume} \qquad f(x) = (1-x)^n \tag{4c}$$

where *f(x)* is referred as a function dependent on the kinetic model of the crystallisation process[30]. If homogeneous nucleation is assumed, the f(x) is taken as $(1 - x)^n$ where *n* is the nucleation order[29]. Hence using the DSC data obtained, a plot of ln(d*x*/d*t*) against ln(1-x) will give a slope equal to *n*, and the value of *A* can be obtained from the intercept and the $\Delta G_c$ evaluated from **eq. (3c)** for the different end temperatures considered. Using these *A* values, the rate constant $(k_n)$ can therefore be estimated according to **eq. (4a).** The unit of $k_n$ is the inverse of time $(s^{-1})$.

*The classic Nyvlt model*: This model is based on the assumption that when nuclei is detectable, the rate of supersaturation is equal to the rate of nucleation. From the classical nucleation theory, the primary number nucleation rate, $J_n$, can be expressed as a function of supersaturation, $\Delta C$[11]:

$$J_n = k_n(\Delta C_{\max})^n \tag{5a}$$

Where $k_n$ is the nucleation rate constant on a number basis, $\Delta C$ the supersaturation and *n* the nucleation order. The unit of $J_n$ is the number of crystals generated per volume and per time. For cooling crystallization, the rate of supersaturation generation is a function of the cooling rate, $\beta$:

$$J_n = \beta\left(\frac{dC_{sat}}{dT}\right) \tag{5b}$$

Where $dC_{sat}/dT$ is the slope of the solubility curve for a given saturation temperature. For the palm oil used in this work, the solubility curve of stearin/olein as a function of temperature (*T* in $^oC$) is given by $C_{sat} = 1\times10^{-6}e^{0.2695T}$. At the point of nucleation, the maximum possible supercooling (or metastable zone width (MSZW)), $\Delta T_{max}$, and the corresponding maximum supersaturation, $\Delta C_{max}$, are given by:

$$\Delta C_{\max} = \Delta T_{\max}\left(\frac{dC_{sat}}{dT}\right) \tag{5c}$$

Combining eq. (5b) and (5c) into eq. 5a results in:

$$\beta\frac{dC_{sat}}{dT} = k_n\left(\frac{dC_{sat}}{dT}\right)^n(\Delta T_{\max})^n$$
$$\beta = k_n\left(\frac{dC_{sat}}{dT}\right)^{n-1}(\Delta T_{\max})^n \tag{5d}$$

The Nyvlt model effectively relates the effect of cooling rate ($\boldsymbol{\beta}$) with the metastable zone width ($\boldsymbol{\Delta T_{max}}$) at a particular operating condition as (see Nyvlt[31] and Sangwal[32] for full derivation of this model):

$$\ln \beta = +\ln(k_n) + (n-1)\ln\left(\frac{dC_{sat}}{dT}\right) + n\ln(\Delta T_{\max}) \quad (5e)$$

As a result from a plot of $\ln(\beta)$ against $\ln(\Delta T_{max})$, the nucleation order ($n$) and the nucleation rate constant ($k_n$) can be estimated from the slope and the intercept of the plot respectively. For number basis, the unit of $k_n$ is the inverse of time ($s^{-1}$).

In summary, the Avrami model evaluates the *overall* crystallisation rate constant ($s^{-n}$) and the crystallisation growth mechanism at isothermal conditions; the F-T model estimates the nucleation rate ($s^{-1}$) from the activation energy required for nucleation at a given temperature and finally, the Nyvlt model predicts both the nucleation rate ($s^{-1}$) and the nucleation order at non-isothermal conditions.

## III. DATA FOR MODELS

For the palm oil, the solid phase is the *stearin* while the liquid phase is *olein*, which are represented in the cooling and melting thermograms (DSC output – the indication of enthalpy change as a function of temperature) obtained from the dynamic DSC analysis. The cooling thermogram (**Fig 1**) shows two distinct exothermic peaks: the one at a low temperature (-4.5°C) corresponds to the low melting fraction (*olein*) due to its high degree of unsaturation; while the second peak at 16°C is associated with the crystallisation of the high melting fractions (*stearin*). The broader peak at this low temperature than at the high temperature indicates a relatively wider range of triglycerides within the temperature region. Similar results were reported in a previous study on RBD palm oil[33].

Likewise, the melting thermogram (**Fig 2**) also shows two groups of endothermic peaks; the peaks at 28°C and 35.5°C correspond to the high melting fractions (stearin) while the low temperature endothermic peaks (4.5°C and 7.5°C) correspond to the low melting fractions (olein); the larger size of this endotherm is consistent with the wider range of low melting fractions discussed earlier.

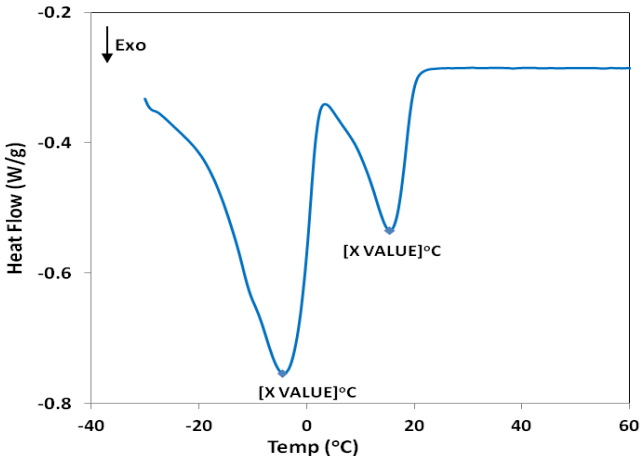


**FIG 1: DYNAMIC COOLING THERMOGRAM OF PALM OIL AND ITS FRACTIONS**

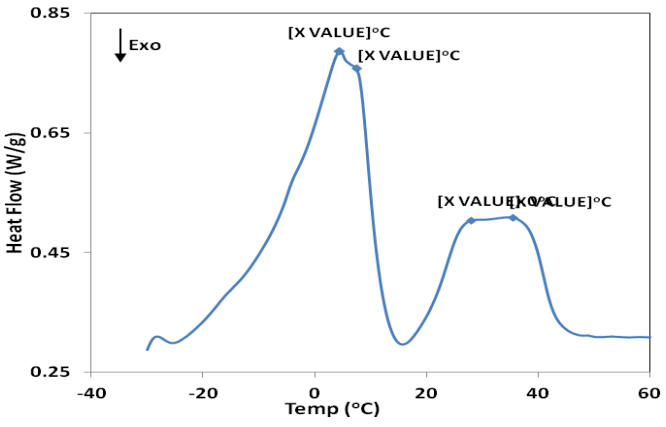


**FIG 2: DYNAMIC MELTING THERMOGRAM OF PALM OIL AND ITS FRACTIONS**

The isothermal crystallisation thermograms at different end temperatures from 293 K to 301 K are shown in **Fig 3** where the heat of crystallisation is plotted as a function of time. It can be seen that the time taken (i.e. induction time, $\tau$) for crystallisation to begin – taken as the onset of the exothermic peak – increased with increasing end temperatures. This can be attributed to reduced degree of supercooling as the higher the end temperature, the closer to the equilibrium temperature the system becomes, hence the lower the driving force for the crystallisation process, as it is case for solution crystallising[34]. Images from the polarised light microscope in **Fig 4** show different crystal morphologies from the samples collected after about 1 hr for the different crystallisation temperatures; for instance, fully-formed spherulitic crystals were observed at 293 K, dendritic spherulites at 303 K and a developing spherulites at 298 K, which supports only one morphology at a given crystallisation temperature studied.

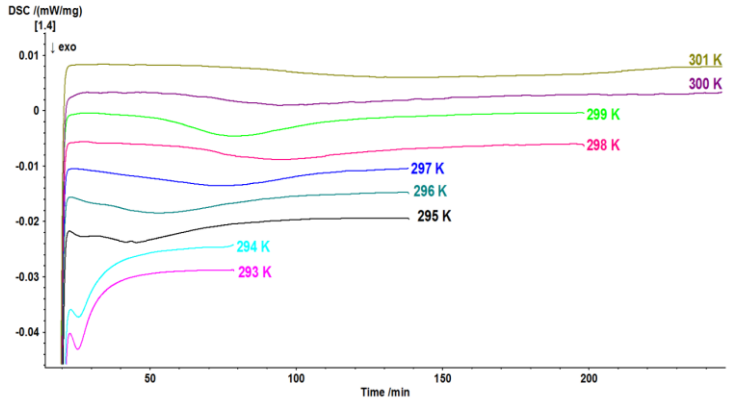


**FIG 3. ISOTHERMAL CRYSTALLISATION THERMOGRAM SHOWING THE INDUCTION TIME AT DIFFERENT END TEMPERATURES**

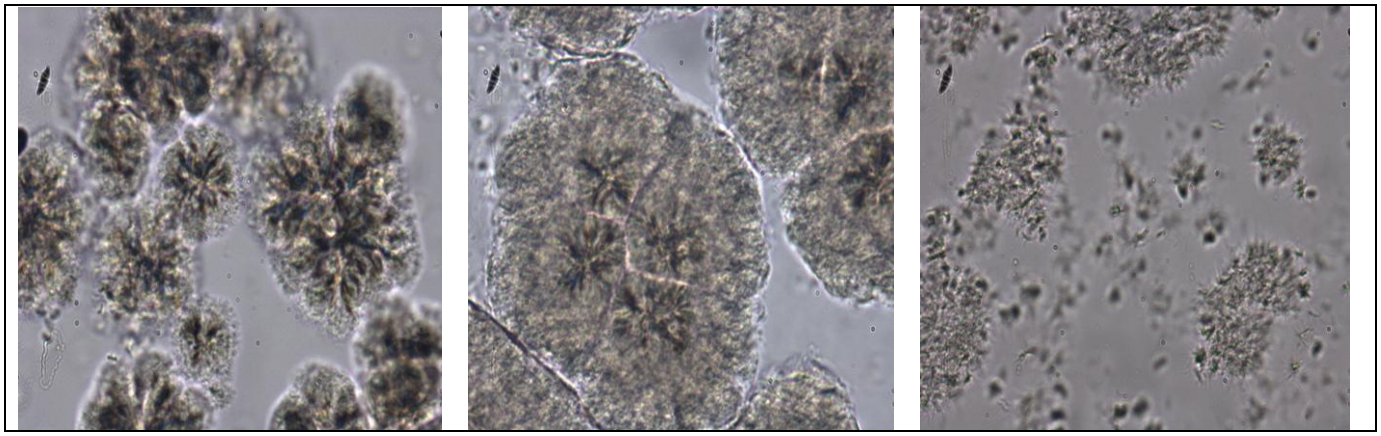

**FIG 4: MICROSCOPIC IMAGES OF PALM STEARIN CRYSTALS AT 293 K (A), 298 K (B) AND 303 K (C)**

## IV. DISCUSSION

### 4.1 The Avrami model

Using the DSC isothermal crystallisation thermograms and the induction time analysis, a plot of the solid fraction (***x***) against time (***t***) is shown in **Fig 5** with the well-known sigmoid curve for isothermal fat crystallisation. The changing gradient of the curve depicts the initial formation of nuclei, followed by a rapid crystal growth, then the slowing down by impingement due to colliding crystal faces[2, 35], as indicated on the right of **Fig. 5**. These stages are relatively more defined as "*S*" shaped curves at the higher temperatures (≥296 K) due to the faster crystallisation rate at low temperatures in a previous study by Zhang *et al*[36].

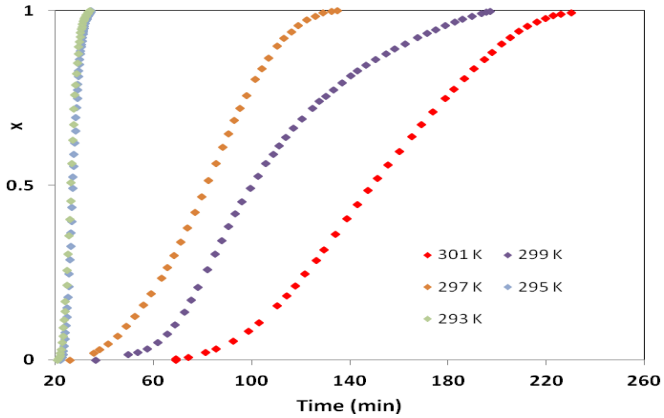


**FIG 5: PERCENTAGE OF SOLID FAT FRACTION WITH TIME AT DIFFERENT CRYSTALLISATION TEMPERATURES**

By plotting ln[-ln(1–*x*)] against ln(*t*) from the Avrami analysis, ***x*** values between 25% and 75%[4] are displaced as a function of the crystallisation time in **Fig 6** a good linear relationship ($R^2 > 0.99$) indicating the applicability of the model to the fat system used in this study. The resultant ***n*** and ***k*** values are listed in **Table 1.** It can be seen from this table that the Avrami exponent (***n***) for the palm oil used in this study was relatively unaffected by the end crystallisation temperatures within the range considered, as it was relatively constant (2.5±0.2, P > 0.05 using ANOVA with single factor analysis). The ***n*** value is an indication of the growth mechanism of the crystals formed according to Kawamura[37] and Wright *et al*[38], which ranges from *rod-like* for n = 1 to *polyhedral* growth (three-dimensional) for n = 4. For polymer and organics systems, an *n* value of 2 or 3 indicates one or two dimensional nucleation of the crystal nucleus; a range of 3.85 to 4.49 has been reported for polyethylene oxide. From n ≈ 3 in this study, the crystal growth mechanism can be taken as *plate-like* (i.e. two-dimensional growth). However previous studies have reported ***n*** values greater than 4 for palm oil crystallisation which was attributed to sporadic and heterogeneous nucleation. This discrepancy could be caused by different triglyceride compositions and different cooling rates of the DSC analyses used (unpublished work by Toro-Vazquez *et al*[39]). For the estimated overall rate constant (***k***) also shown in Table 1, it generally decreases with increasing end temperatures, indicating a slower crystallisation process at higher temperatures as expected[34]. The sharp increase in the k value from 296 K to lower temperatures can be linked to polymorphic transition occurring at those temperatures. In summary, the rate constants (k) obtained from this work fall within the similar range as the previous work, suggesting similar crystallisation kinetics [40].

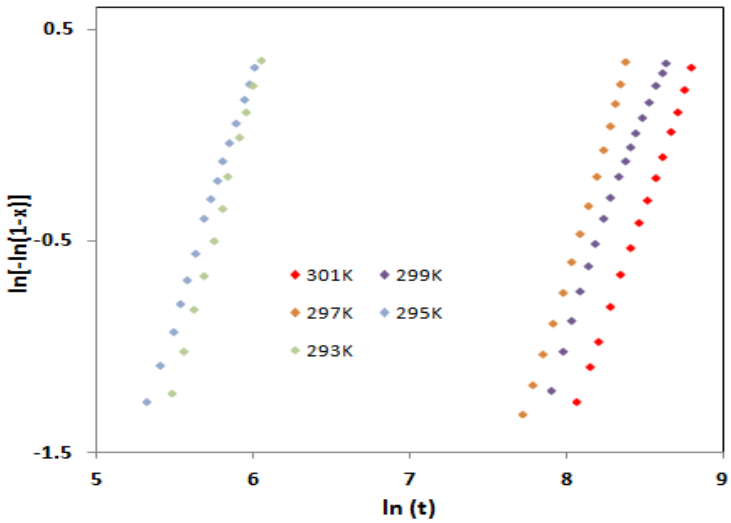


**FIG 6: PLOT FOR AVRAMI MODEL ANALYSIS**

Note that the *n*-dependency of the unit of these ***k*** values ($s^{-n}$) makes it impossible to compare with related values from other models; hence the trend of ***k*** with respect to the end temperatures, as opposed to the actual values, is the key element from this model.

### 4.2 The Fisher-Turnbull model

The results discussed above give an indication of the *overall* crystallisation kinetics. In order to examine the nucleation occurrence, the Fisher-Turnbull equation was used to estimate the activation free energy barrier ($\Delta G_c$) needed for the formation of stable nuclei. The related plot of ($\ln(T\tau)$ against $1/T(\Delta T)^2$) and the calculated values of $\Delta G_c$ together with the estimated nucleation rate constants ($k_n$) using **eq. (4a)** are shown in **Fig 7** and **Table 1** respectively. Note that the melting temperature ($T_m$) used to calculate $\Delta T$ was taken as the peak end temperature of the melting curve shown in **Fig 2** which was 44°C. **Fig 7** effectively displays the relationship between the energy barrier for nucleation (the vertical axis) and the inverse of supersaturation (the horizontal axis); the higher the crystallisation temperature, the larger the energy barrier (higher $\Delta G_c$), again due to lower degree of supercooling at higher end temperatures, which is as expected[41].

**Fig 7** has a good but discontinued linearity from about 298 K. This discontinuity can be attributed to the formation of crystals of different polymorphic states; according to Ostwald's rule of stages[42], nucleation of the less stable polymorph (α) was favoured especially at low end temperatures (higher supersaturation) where nucleation rate is higher with less energy barrier[43]; hence it can be inferred that the crystals formed at T ≥ 298 K is the β polymorph[44]; this trend is similar to results shown in previous studies by Chen *et al*[45] and Ng[46]. The features of the discontinuity and the different nucleation

mechanisms leading to different polymorphs are also clearly shown in **Table 1** where higher nucleation rate constants ($k_n$) were extracted at lower end temperatures and vice versa; the corresponding *n* values (see **eq. 4c**) obtained here was *~1* hence the nucleation process can be taken as a first order.

**TABLE 1**
**KINETICS PARAMETERS FOR ALL MODELS; (TM = 317K)**

| | *Avrami model* | | *Fisher-Turnbull model* | | *Nyvlt model* | |
|---|---|---|---|---|---|---|
| $T_c$ *(K)* | ***n*** | $k \times 10^{10}$ $(s^{-n})$ | $\Delta G_c$*(kJ/mol)* | $k_n \times 10^6$ $(s^{-1})$ | ***n*** | $k_n \times 10^6 (s^{-1})$ |
| 293 | 2.7 ± 0.2 | 2866 | 1.37 | 4188 | 8.97 | 399 |
| 295 | 2.3 ± 0.1 | 1646 | 1.63 | 4158 | | |
| 296 | 2.2 ± 0.0 | 282 | 1.79 | 669 | | |
| 297 | 2.5 ± 0.1 | 12 | 1.98 | 465 | | |
| 299 | 2.3 ± 0.4 | 12 | 4.75 | 476 | | |
| 301 | 2.7 ± 0.4 | 4 | 6.01 | 202 | | |

The property, $\Delta G_d$, being the activation energy for molecular diffusion takes into account the impeded molecular movement due to increased viscosity at low temperatures; hence it is expected that the nucleation rate becomes more influenced by $\Delta G_d$ as the end temperature is reduced[47]. This was however not explored further in this study.

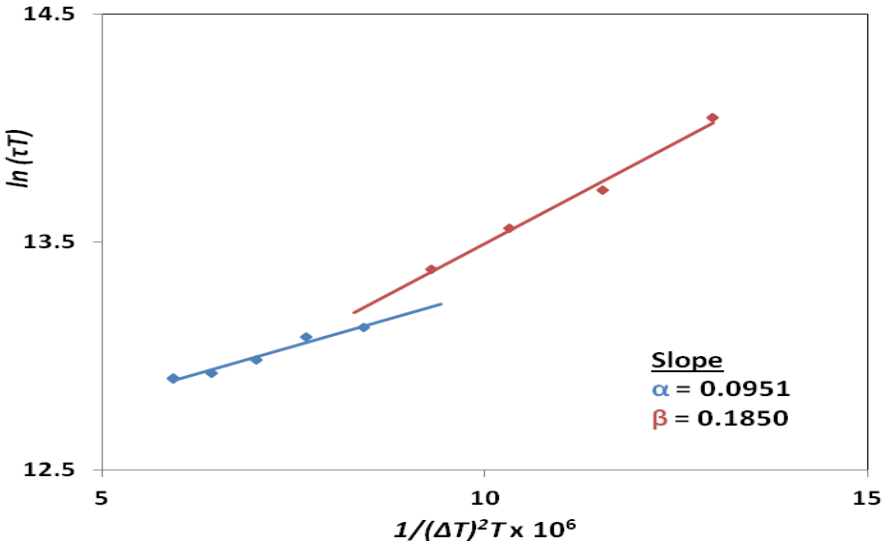


**FIG 7: KINETICS PARAMETER FROM FISHER-TURNBULL EQUATION**

### 4.3 The Nyvlt model

To extract non-isothermal kinetics from the Nyvlt model, the measurements of metastable zone width (MSZW) as a function of cooing rates are required, **Fig 8** shows the typical turbidimetry measurement, with the highest transmittances indicating that the palm oil is completely melted. The moment when the transmittance starts to drop is regarded as the onset of nucleation (i.e. the formation of palm stearin solid crystals). The transmittance keeps decreasing as crystallisation proceeds with more stearin crystals in the system until the signals level off to zero or close to zero indicating the end of the crystallisation process. The 'dissolution' profile was obtained by reheating the system from the end temperature (20°C) back to the start temperature (50°C). In this way, the metastable zone width (MSZW) can be determined as the difference between the 'dissolution' and the crystallisation temperatures at each of the cooling rates. **Table 2** lists the MSZW for the three cooling rates investigated; as expected that the highest cooling rate (1.0°C/min) has the lowest nucleation temperature hence the largest MSZW due to rapid supercooling and longer nuclei stability period[48-50]; similar results were reported in previous

studies relating to the effects of cooling rate on fat crystallisation[1, 51]. This is also consistent with the results from the DSC isothermal analysis (**Fig 3**) discussed earlier in that the crystallisation rate is higher at lower end temperatures.

By plotting $ln(\beta)$ against $ln(\Delta T_{max})$, the nucleation order (***n***) and the nucleation rate constant ($k_n$) can be evaluated according to **eq. (5e)** and are also shown in **Table 1**. Values of *n* between 6.0 and 16 were reported for fat systems of different tripalmiltin concentrations in a previous study[51], and the value derived from this study (~9) is within this range. The $k_n$ value obtained here ($3.99 \times 10^{-4}$ $s^{-1}$) is a lot lower than those reported for solution crystallisation of organics (e.g. adipic acid) in a previous study[52], and this may be attributed to the relatively slower rate of molecular growth to a stable nuclei for triglyceride systems due to the high viscosity; a higher nucleation order (~9) also supports the influence of mass transfer on melt crystallisation[53].

**TABLE 2**
**MSZW VALUES FOR DIFFERENT COOLING RATES**

| β (°C/min) | $T_{cry}$ (°C) | $T_{dis}$ (°C) | $\Delta T_{max}$ (°C) |
|---|---|---|---|
| 1.0 | 24.2 ± 0.2 | 45.1 ± 0.1 | 21.0 ± 0.2 |
| 0.5 | 25.2 ± 0.3 | | 19.9 ± 0.4 |
| 0.25 | 27.2 ± 0.4 | | 17.9 ± 0.4 |

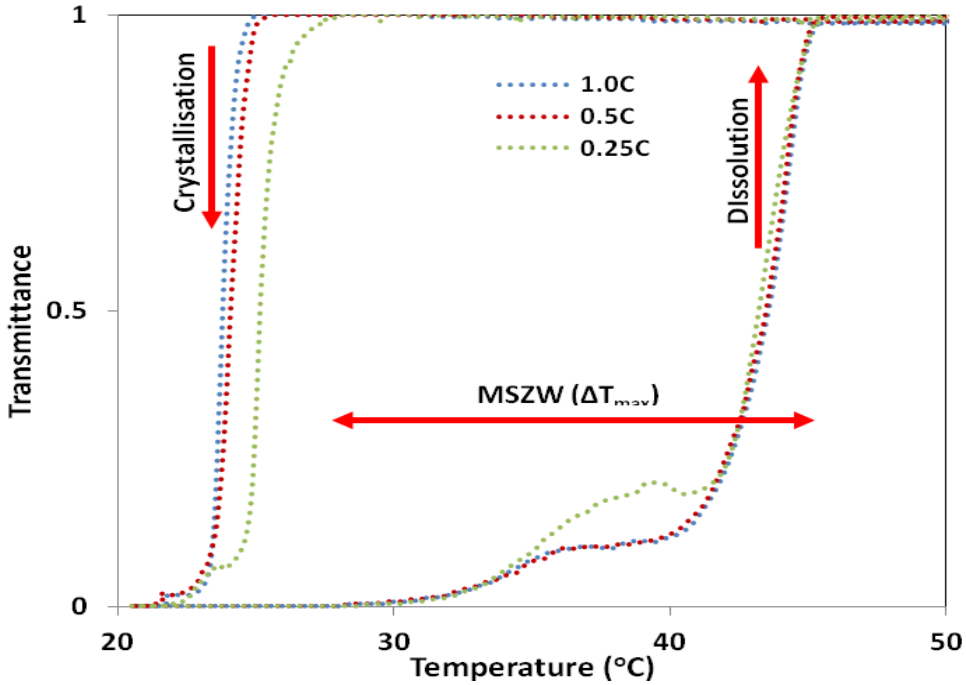


**FIG 8. TURBIDITY MEASUREMENTS FOR MSZW DETERMINATION AT DIFFERENT COOLING RATES**

### 4.4 Comparison of models

Comparing the nucleation rate constants evaluated between the Fisher-Turnbull and the Nyvlt models (see in **Table 1**), the Nyvlt non-isothermal nucleation rate constant is of similar order of magnitude to the Fisher-Turnbull isothermal ones for the higher end temperatures (298 – 300 K), while of an order of magnitude lower for the lower end temperatures. The values themselves match reasonably well for the cooling rates investigated, giving the fact that the model assumptions are widely different, where the Nyvlt model took a polythermal approach to estimating the kinetic parameters, assuming that supersaturation rate corresponds to nucleation rate from the onset of nuclei formation and there is no growth in nuclei[54], while the Fisher-Turnbull model was based on isothermal conditions with homogenous nucleation being assumed in the crystallisation process. The two models can be used for estimating nucleation parameters for both melts and organics.

The dependency of the ***k*** values on the growth mechanism (**n**) evaluated from the Avrami model together with the fact that it describes the *overall* crystallisation rate makes any comparison irrelevant. Furthermore the growth mechanism (**n**) from the

Avrami model has a completely different definition from the apparent nucleation order predicted from the Nyvlt model which is dependent on the formation process of stable nuclei[32], once again no comparison is possible.

## V. CONCLUSION

In this work we use the crystallisation of palm oil (a typical melt) as the model process and evaluated the kinetic parameters using three model approaches: two from the traditional melt fractionation, one from the classic solution crystallisation. The objective was to establish critical understanding on the various model approaches and their applications. Our results show that the Fisher-Turnbull and the Nyvlt models are useful in estimating the nucleation rate constants ($k_n$) with reasonable agreement: this unites the model approaches and allows comparison between fat fractionation and solution crystallisation. The lower rate constants predicted from the melt crystallisation in comparison to that from the solution crystallisation of organics are expected and resulted from the high viscosity that impedes the growth of nuclei to a stable size.

While the Avrami model is capable of evaluating the growth mechanism of the formed crystals ($n$) and the *overall* crystallisation rate constant ($k$), none of the parameters can be compared with other models because of the different definition of the growth mechanism as well as the dependence of k value on the growth mechanism when dealing different fats of varying compositions.

Finally, the end temperatures and cooling profiles are the essential operational parameters that can be explored in order to obtain crystal product of desired physical properties.

## ACKNOWLEDGEMENTS

The authors would thank CMAC for funding this project and AarhusKarlshamn (AAK) for supplying the palm oils used in the experiments carried out. Finally, much appreciation goes to B P Chow who was available to offer technical advice when required.

## REFERENCES

[1] Geoff, T., K.W. Smith, and F.W. Cain, *Solvent Fraction of Palm Oil*, in *International News on Fats, Oils and Related Materials : INFORM*. 2006, AOCS Press. p. 324-326.

[2] Foubert, I., K. Dewettinck, and P.A. Vanrolleghem, *Modelling of the crystallization kinetics of fats.* Trends in food science & technology, 2003. **14**(3): p. 79-92.

[3] Avrami, M., *Kinetics of phase change. I General theory.* The Journal of Chemical Physics, 1939. **7**(12): p. 1103-1112.

[4] Avrami, M., *Kinetics of phase change. II transformation-time relations for random distribution of nuclei.* The Journal of Chemical Physics, 1940. **8**(2): p. 212-224.

[5] Marangoni, A.G., *Fat crystal networks*. Vol. 140. 2004: CRC Press.

[6] Mazzanti, G., A.G. Marangoni, and S.H. Idziak, *Modeling phase transitions during the crystallization of a multicomponent fat under shear*. Physical Review E, 2005. **71**(4): p. 041607.

[7] Khanna, Y.P. and T.J. Taylor, *Comments and recommendations on the use of the Avrami equation for physico-chemical kinetics.* Polymer Engineering & Science, 1988. **28**(16): p. 1042-1045.

[8] Himawan, C., V. Starov, and A. Stapley, *Thermodynamic and kinetic aspects of fat crystallization.* Advances in colloid and interface science, 2006. **122**(1): p. 3-33.

[9] Takeuchi, M., S. Ueno, and K. Sato, *Crystallization kinetics of polymorphic forms of a molecular compound constructed by SOS (1, 3-distearoyl-2-oleoyl-sn-glycerol) and SSO (1, 2-distearoyl-3-oleoyl-rac-glycerol).* Food Research International, 2002. **35**(10): p. 919-926.

[10] Söhnel, O. and J.W. Mullin, *Interpretation of crystallization induction periods.* Journal of Colloid And Interface Science, 1988. **123**(1): p. 43-50.

[11] Mullin, J.W., *5 - Nucleation*, in *Crystallization (Fourth Edition)*. 2001, Butterworth-Heinemann: Oxford. p. 181-215.

[12] Ng, W., *A study of the kinetics of nucleation in a palm oil melt.* Journal of the American Oil Chemists' Society, 1990. **67**(11): p. 879-882.

[13] Dodd, J.W., K.H. Tonge, and B.R. Currell, *Thermal methods.* 1987.

[14] Nassu, R.T. and L.A. Guaraldo Gonçalves, *Determination of melting point of vegetable oils and fats by differential scanning calorimetry (DSC) technique.* Grasas y Aceites, 1999. **50**(1): p. 16-21.

[15] Evans, U.R., *The laws of expanding circles and spheres in relation to the lateral growth of surface films and the grain-size of metals.* Transactions of the Faraday Society, 1945. **41**(0): p. 365-374.

[16] Meares, P., *Polymers: structure and bulk properties*. 1965: Van Nostrand Reinhold.

[17] Hay, J., *Application of the modified avrami equations to polymer crystallisation kinetics.* British Polymer Journal, 1971. **3**(2): p. 74-82.

[18] Sperling, L., *Introduction to physical polymer science, 1992*. John Wiley & Sons, New York.

[19] Cazé, C., et al., *A new method to determine the Avrami exponent by d.s.c. studies of non-isothermal crystallization from the molten state.* Polymer, 1997. **38**(3): p. 497-502.

[20] Lu, M.G., M.J. Shim, and S.W. Kim, *Dynamic DSC Characterization of Epoxy Resin by Means of the Avrami Equation.* Journal of Thermal Analysis and Calorimetry. **58**(3): p. 701-709.

[21] Bhattacharyya, A.R., et al., *Crystallization and orientation studies in polypropylene/single wall carbon nanotube composite.* Polymer, 2003. **44**(8): p. 2373-2377.

[22] Wang, X. and J.J. Vlassak, *Crystallization kinetics of amorphous NiTi shape memory alloy thin films.* Scripta Materialia, 2006. **54**(5): p. 925-930.

[23] Campos, R., S. Narine, and A. Marangoni, *Effect of cooling rate on the structure and mechanical properties of milk fat and lard.* Food Research International, 2002. **35**(10): p. 971-981.

[24] Galwey, A.K. and M.E. Brown, *Thermal decomposition of ionic solids: chemical properties and reactivities of ionic crystalline phases*. Vol. 86. 1999: Elsevier.

[25] Sharples, A., *Introduction to polymer crystallization.* 1966.

[26] Pal, S. and A.K. Nandi, *Cocrystallization mechanism of poly(3-alkyl thiophenes) with different alkyl chain length.* Polymer, 2005. **46**(19): p. 8321-8330.

[27] Henderson, D.W., *Thermal analysis of non-isothermal crystallization kinetics in glass forming liquids.* Journal of Non-Crystalline Solids, 1979. **30**(3): p. 301-315.

[28] Becker, R., *Die Keimbildung bei der Ausscheidung in metallischen Mischkristallen.* Annalen der Physik, 1938. **424**(1-2): p. 128-140.

[29] Vyazovkin, S., *Isoconversional Kinetics of Thermally Stimulated Processes*. 2015: Springer International Publishing.

[30] Michèle, P., F. Loïc, and S. Michel, *From the drawbacks of the Arrhenius-f (α) rate equation towards a more general formalism and new models for the kinetic analysis of solid–gas reactions.* Thermochimica Acta, 2011. **525**(1): p. 93-102.

[31] Nývlt, J., *Kinetics of nucleation in solutions.* Journal of Crystal Growth, 1968. **3–4**(0): p. 377-383.

[32] Sangwal, K., *A novel self-consistent Nývlt-like equation for metastable zone width determined by the polythermal method.* Crystal Research and Technology, 2009. **44**(3): p. 231-247.

[33] Che Man, Y.B., et al., *Composition and thermal profile of crude palm oil and its products.* Journal of the American Oil Chemists' Society, 1999. **76**(2): p. 237-242.

[34] Ni, X. and A. Liao, *Effects of mixing, seeding, material of baffles and final temperature on solution crystallization of l-glutamic acid in an oscillatory baffled crystallizer.* Chemical Engineering Journal, 2010. **156**(1): p. 226-233.

[35] Chiang, C.-Y., V. Starov, and D. Lloyd, *Crystallization kinetics of a polymer-solvent system. I: Derivation of model equations.* Colloid journal of the Russian Academy of Sciences, 1995. **57**(5): p. 715-724.

[36] Zhang, X., et al., *Comparative Analysis of Thermal Behavior, Isothermal Crystallization Kinetics and Polymorphism of Palm Oil Fractions.* Molecules, 2013. **18**(1): p. 1036-1052.

[37] Kawamura, K., *The DSC thermal analysis of crystallization behavior in palm oil.* Journal of the American Oil Chemists' Society, 1979. **56**(8): p. 753-758.

[38] Wright, A.J., et al., *The effect of minor components on milk fat crystallization.* Journal of the American Oil Chemists' Society, 2000. **77**(5): p. 463-475.

[39] Toro-Vazquez, J., et al., *Crystallization kinetics of palm stearin in blends with sesame seed oil.* Journal of the American Oil Chemists' Society, 2000. **77**(3): p. 297-310.

[40] Pereira, R.P. and A.M. Rocco, *Nanostructure and crystallisation kinetics of poly (ethylene oxide)/poly (4-vinylphenol-co-2-hydroxyethyl methacrylate) blends.* Polymer, 2005. **46**(26): p. 12493-12502.

[41] Kloek, W., P. Walstra, and T. van Vliet, *Crystallization kinetics of fully hydrogenated palm oil in sunflower oil mixtures.* Journal of the American Oil Chemists' Society, 2000. **77**(4): p. 389-398.

[42] Garti, N. and K. Sato, *Crystallization Processes in Fats and Lipid Systems*. 2001: Taylor & Francis.

[43] Kellens, M. *Developments in fat fractionation technology*. in *Fats and oils and fats group symposium*. 1994. London: Society of Chemical Industry.

[44] Sato, K. and T. Kuroda, *Kinetics of melt crystallization and transformation of tripalmitin polymorphs.* Journal of the American Oil Chemists' Society, 1987. **64**(1): p. 124-127.

[45] Chen, C., et al., *Isothermal crystallization kinetics of refined palm oil.* Journal of the American Oil Chemists' Society, 2002. **79**(4): p. 403-410.

[46] Ng, W.L., *A study of the kinetics of nucleation in a palm oil melt.* Journal of the American Oil Chemists' Society, 1990. **67**(11): p. 879-882.

[47] Turnbull, D. and J.C. Fisher, *Rate of Nucleation in Condensed Systems.* The Journal of Chemical Physics, 1949. **17**(1): p. 71-73.

[48] De Graef, V., et al., *Crystallization behavior and texture of trans-containing and trans-free palm oil based confectionery fats.* Journal of Agricultural and Food Chemistry, 2007. **55**(25): p. 10258-10265.

[49] Cheon, Y.-H., K.-J. Kim, and S.-H. Kim, *A study on crystallization kinetics of pentaerythritol in a batch cooling crystallizer.* Chemical Engineering Science, 2005. **60**(17): p. 4791-4802.

[50] Ni, X. and A. Liao, *Effects of Cooling Rate and Solution Concentration on Solution Crystallization of l-Glutamic Acid in an Oscillatory Baffled Crystallizer.* Crystal Growth & Design, 2008. **8**(8): p. 2875-2881.

[51] Smith, K.W., F.W. Cain, and G. Talbot, *Crystallisation of 1, 3-dipalmitoyl-2-oleoylglycerol and tripalmitoylglycerol and their mixtures from acetone.* European Journal of Lipid Science and Technology, 2005. **107**(9): p. 583-593.

[52] Brown, C.J., et al., *Evaluation of crystallization kinetics of adipic acid in an oscillatory baffled crystallizer.* CrystEngComm, 2014. **16**(34): p. 8008-8014.

[53] Ghotra, B.S., S.D. Dyal, and S.S. Narine, *Lipid shortenings: a review.* Food Research International, 2002. **35**(10): p. 1015-1048.

[54] Nývlt, J., *Induction period of nucleation and metastable zone width.* Collection of Czechoslovak chemical communications, 1983. **48**(7): p. 1977-1983.